Qubit read-out with quantum chaos detector

Dima Shepelyansky (CNRS Toulouse)
www.quantware.ups-tlse.fr/dima

with Klaus Frahm (LPT, Univ. Paul Sabatier, Toulouse)

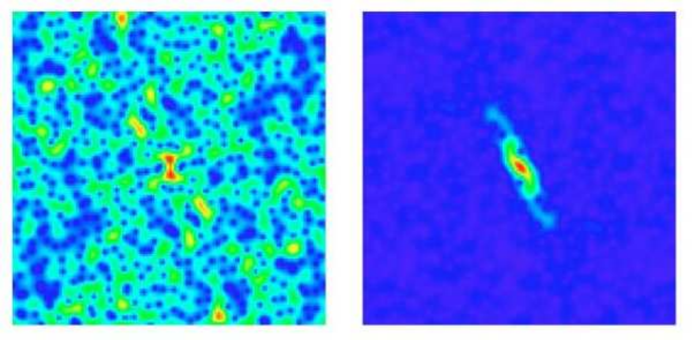

Husimi function of quantum chaos detector for qubit-up/down (left/right)

Phys. Rev. A **72**, 012310 (2005) EC IST-FET Open EDIQIP project
Support: ANR OCTAVES + LABEX NANOX MTDINA project (disruptive)

Transmon with phase modulation

The Hamiltonian is that of a periodically driven pendulum [9] and can be written in the form

$$H = p^2/2 - k\cos(\phi - \lambda \sin t)\,, \qquad (1)$$

where time is rescaled to make $\Omega = 1$, and ϕ is related to φ via $\phi(t) = \varphi(t) + (2eI_0/\hbar C\Omega^2)\sin\Omega t$. The momentum $p = \dot{\phi} = 2eV/\hbar\Omega$ is connected with the total voltage drop V_t across the junction by $V_t = V - (I_0/C\Omega)\cos\Omega t$. The two parameters $k = 2eI_J/\hbar C\Omega^2$ and $\lambda = 2eI_0/\hbar C\Omega^2$ describe the classical system. I_J is the amplitude of the Josephson supercurrent $I_S = I_J \sin\varphi$. The quantized system contains a third dimensionless constant $\not{k} = (2e)^2/\hbar C\Omega$ via the commutator $[p,\phi] = -i\not{k}$. In our units $\not{k}$ plays the role of Planck's constant and corresponds to one quantum of voltage $2e/C$.

Graham, Schlautmann, DS PRL (1991) for Josephson junction;
Graham, Schlautmann, Zoller PRA (1992) for cold atoms in optical lattice

Reduction to the Chirikov standard map

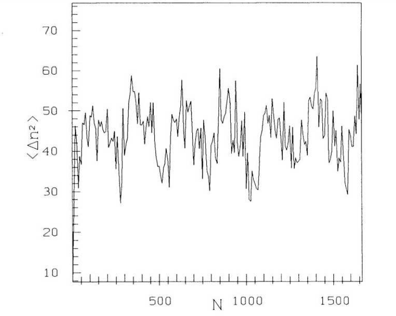

FIG. 1. Mean square of the number of occupied levels of the cosine potential vs the number N of cycles of the external current for $\lambda = 85.0$, $k = 15.0$, and $\bar{k} = 1.58$.

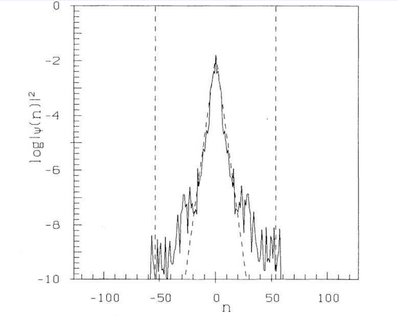

FIG. 2. Logarithm of the time-averaged occupation probability corresponding to Fig. 1. Dashed lines give the border $|n| = \lambda/\bar{k}$ of the classical chaotic domain and the exponential falloff with the localization length l_D.

fast resonance ($d\phi/dt = \lambda \cos t$) crossing regime $\lambda/k \gg 1$ or $I_0 \gg I_J$ ($|p| < \lambda$)
$\bar{p} = p - 2\sqrt{\pi}(k/\sqrt{\lambda})\sin\phi$, $\bar{\phi} = \phi + 2\pi\bar{p}$ => $\bar{p} = p + K\sin x, \bar{x} = x + \bar{p}$
Chaos border $k > \sqrt{\pi\lambda}/40$; diffision $D = (\Delta p)^2/t \approx k^2/\lambda$ in the range $|p| < \lambda$
or $< V^2 >^{1/2} \approx I_0/(\sqrt{3}C\Omega) \propto \lambda$
Dynamical (Anderson) localization of diffusion: $\ell_D = 2\pi D/\hbar_{eff}{}^2 \propto 1/\lambda$,
$\hbar_{eff} = 4e^2/(\hbar C\Omega)$ (k-bar); $p = \hbar_{eff} n$, $|\psi| \sim \exp(-|n|/\ell_D)$

Transmon chaos vs quantum localization

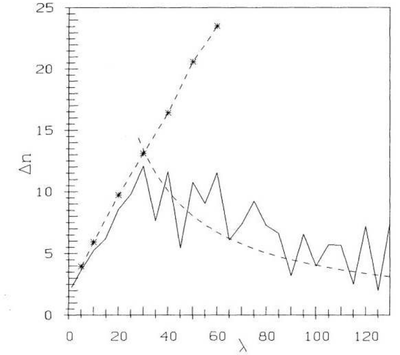

FIG. 3. Root mean square of the number of occupied levels versus the normalized amplitude λ of the driving current for the same values of the parameters k,$\bar{k}$ as in Fig. 1. Classical results, indicated by ∗'s, are joined by a dashed line. Another dashed line gives the analytical result for the quantum regime.

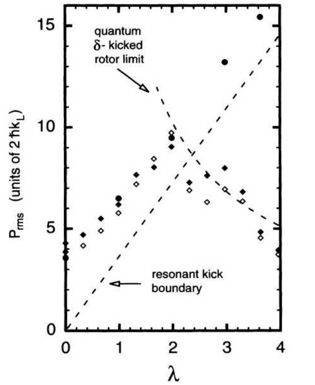

FIG. 1. rms momentum spread in units of $2\hbar k_L$ as a function of λ. The parameters for this curve are $\Omega_{\text{eff}}/2\pi = 22$ MHz (rms), $\delta_L/2\pi = 5.4$ GHz, $\omega_m/2\pi = 1.3$ MHz, $k = 0.34$ (rms), and $\bar{k} = 0.16$. The straight and curved dashed lines denote the resonant kick boundary and the quantum δ-kicked rotor limit, respectively. The data are given for a duration of 10 μs (empty diamonds) and 20 μs (solid diamonds) and show that saturation has been reached. The solid circles are the result of a classical simulation and show agreement with the data up to a critical value of λ. Note that there are no adjustable parameters in this comparison between theory and experiment. The dominant

Left: theory for JJ Graham et al. PRL (1991); right: Raizen et al. experiment with cold atoms in modulated optical lattice PRL (1994)

Chirikov standard map quantized

classical Hamiltonian and map:

$H(p,x) = p^2/2 + K \cos x \sum_m \delta(t-m)$

$\bar{p} = p + K \sin x \ , \quad \bar{x} = x + \bar{p}$

Chaos border: $K > 0.9716...$, diffusion $D = p^2/t \approx K^2/2$;

Kolmogorov-Sinai entropy (Lyapunov exponent) $\lambda \approx \ln(K/2)$

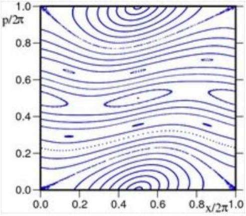

Figure 1: K=0.5

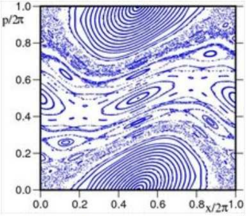

Figure 2: K=0.971635

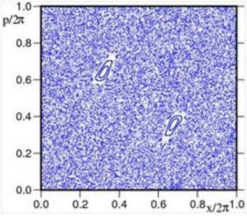

Figure 3: K=5

Quantum kicked rotator or kicked transmon:

Chirikov (1969), Chirikov (1979), Chirikov, Izrailev, DS (1981), DS (1987)

$\bar{\psi} = \exp(-ip^2/2\hbar) \exp(-iK/\hbar \cos x)\psi = U_S \psi$

commutator $[p,x] = -i\hbar$ ($k = K/\hbar$; $T = \hbar$; $K = kT$

dynamical localization: $\ell \approx D/\hbar^2 = k^2/2$; $\psi \propto \exp(-|n-n_m|/\ell)$

Experimental observation of localization with cold atoms in kicked optical lattice: Raizen et al. PRL (1995)

Quantum chaos detector

$H = p^2/2 + [K + \epsilon_c \sigma_z] \cos\theta \sum_m \delta(t-m) + \delta\sigma_x$

Decay rates of density matrix elements:

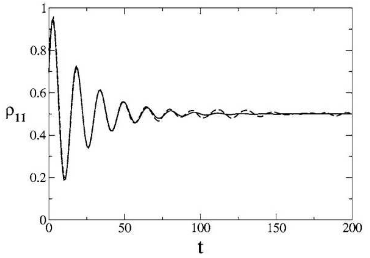

FIG. 4. Population relaxation, that is, evolution in time of ρ_{11} (solid curve). Parameter values are as in Fig. 1. The dashed curve shows the fit $\rho_{11}=\frac{1}{2}+a\sin(bt+\phi)\exp(-\Gamma_1 t)$, with $a=0.5$, $b=0.404$, $\phi=0.405$, and $\Gamma_1=4.36\times10^{-2}$.

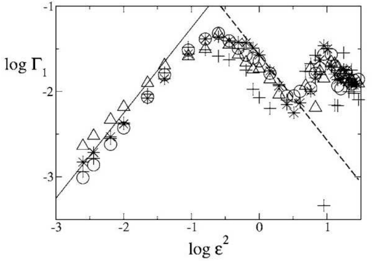

FIG. 5. Dependence of the relaxation rate Γ_1 on the coupling strength ϵ, at $\delta=0.1$, $K=8$, $\hbar=4.91\times10^{-2}$ (plus), $\hbar=1.23\times10^{-2}$ (triangles), $\hbar=3.07\times10^{-3}$ (circles), and $\hbar=7.67\times10^{-4}$ (stars). The initial state of the qubit is $|\psi_s\rangle=(|0\rangle+2|1\rangle)/\sqrt{5}$. The straight lines show $\Gamma_1=A\epsilon^2$, with $A=0.56$ (solid line) and $\Gamma_1=B/\epsilon^2$ with $B/\delta^2=2.7$ (dashed line).

small coupling ϵ: $\Gamma_1 \approx \Gamma_2 \approx \epsilon^2/2$, quantum Zeno effect: $\Gamma_1 \sim \delta^2/\Gamma_2 \sim \Delta^2/\epsilon^2$ (omic dissipation e.g. Makhlin et al. RMP **73**, 257 (2001))

similar dependece of $\Gamma_{1,2}$ for qubit coupled to quantum dot or SYK black hole with quantum chaos: Frahm, DS EPJB (2018)

Quantum chaos detector: Lyapunov regime

Decay rates of density matrix elements:
decay with Lyapunov exponent $\lambda \approx \ln(K/2) = 0.81$

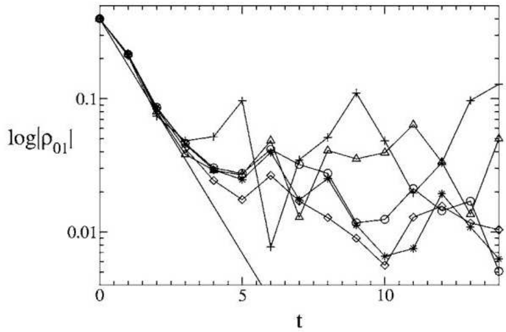

FIG. 7. Time dependence of $|\rho_{01}|$ for $K=4.5$, $\epsilon_c \equiv \epsilon 2\pi/2^{n-1} = 0.8$, and $\delta=0.01$. The initial state of the qubit is $|\psi_s\rangle = (|0\rangle + 2|1\rangle)/\sqrt{5}$, the initial detector state is a Gaussian wave packet with area size $\hbar$ centered at $p=0$, $\theta=\pi$. Data are shown for $\hbar=4.91\times10^{-2}$ (plus), $\hbar=1.23\times10^{-2}$ (triangles), $\hbar=3.07\times10^{-3}$ (circles), $\hbar=7.67\times10^{-4}$ (stars), and $\hbar=1.92\times10^{-4}$ (diamonds). The straight line represents the exponential decay with rate given by the Lyapunov exponent $\lambda \approx \ln(K/2)=0.81$ [33].

Quantum chaos efficient detection

Vicinity of bifurcation point at $K = 4$, $N_d = 12$

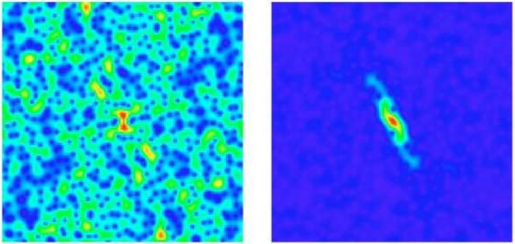

FIG. 8. (Color online) Husimi function in action-angle variables (p,θ) for the detector, with $-\pi \leqslant p < \pi$ (vertical axis) and $0 \leqslant \theta < 2\pi$ (horizontal axis) for the kicked rotator coupled to up spin (left) and down spin (right), at $K=4.5$, $\epsilon_c=0.8$, $\delta=0.1$, $\hbar=1.23 \times 10^{-2}$, $t=20$. The initial states of the kicked rotator and the qubit are a Gaussian packet centered at the fixed point $p=0$, $\theta=\pi$ and $|\psi_s\rangle=(|0\rangle+|1\rangle)/\sqrt{2}$. Color represents the density from blue/black (minimal value) to red/gray (maximal value).

Quantum chaos non-efficient detection

Chaotic regime $K = 8$, $N_d = 12$

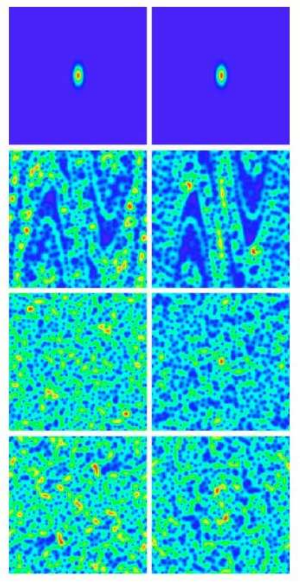

FIG. 10. (Color online) Hypersensitivity of the Husimi function on the spin value for $K=8$, $\epsilon=0.4$, $\delta=0.2$, and $\hbar=1.23\times10^{-2}$. From top to bottom $t=0, 4, 8, 12$. The left plots are for up spin, the right ones for down spin. The initial states of the kicked rotator and of the qubit are a Gaussian packet centered at the fixed point $p=0$, $\theta=\pi$ and $|\psi_s\rangle=(|0\rangle+|1\rangle)/\sqrt{2}$. The color code is as in Fig. 8.

Transmon (pendulum) Separatrix detector and quantum synchronization of qubits

* Hamiltonian $H = p^2/2 + (K + \epsilon_c \sigma_z) \cos x + \delta \sigma_x$

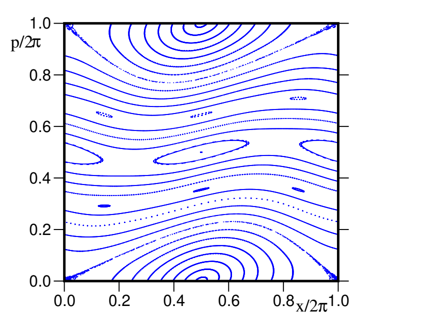

close to experiment (standard map $K = 0.5 \ll 1$)
Lescanne et al. Phys. Rev. Appl. **11**, 014030 (2019)

* Quantum synchronization and entanglement of qubits coupled to a driven dissipative resonator
Zhirov, DS PRL (2008), PRB (2009); Chepelianskii, DS (in progress)

Quantum strange attractor

quantum dissipative map with quantum trajectories

$\bar{p} = (1-\gamma)p + K \sin x\ , \quad \bar{x} = x + \bar{p}; \qquad [\hbar = 0.012, \gamma = 0.5, K = 7]$

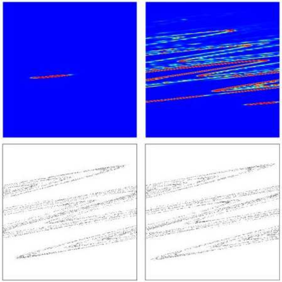

FIG. 1 (color online). Top: Husimi functions in phase space for a single quantum trajectory taken after $t = 300$ kicks, at $K = 7$, $\hbar = 0.012$, $\gamma = 0.5$ (left), and $\gamma = 0.01$ (right). Here x (horizontal axis) and p (vertical axis) vary in the intervals: $0 \le x < 2\pi$, $-25 \le p \le 25$ (left), and $-100 \le p \le 50$ (right); the width of the p interval is the same in both cases for comparison purposes. The initial Gaussian wave packet is located at $(\langle x \rangle, \langle p \rangle) = (5\pi/4, 0)$. The color is proportional to density: blue for zero and red for maximum. Bottom: quantum Poincaré section (left), obtained from average quantum x, p values for the case of top left panel and its classical counterpart (right); here $0 \le x < 2\pi$ and $-15 \le p \le 15$.

Ehrenfest explosion (or collapse) of wave packet $t_E \sim |\ln \hbar|/\lambda < 1/\gamma$:

Carlo, Benenti, DS PRL **95**, 164101 (2005)

OCTAVES publications of Toulouse node

Refs:

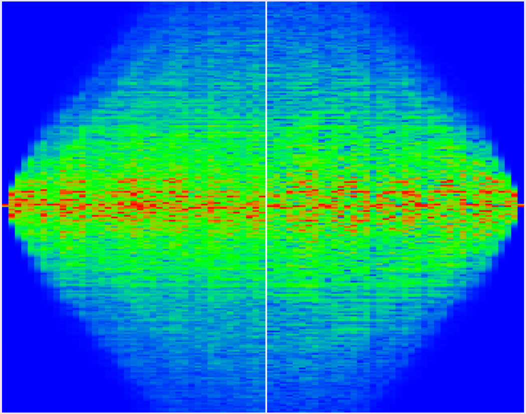

T1) K.M.Frahm and D.L.Shepelyansky, "Chaotic Einstein-Podolsky-Rosen pairs, measurements and time reversal", Eur. Phys. J. D v.75, p. 277(2021)

T2) L.Ermann, K.M.Frahm and D.L.Shepelyansky, "Loschmidt echo and Poincare recurrences of entanglement", submitted to J. Phys. A on 7 Jan (2022) (arXiv:2201.02600[quant.ph])